

NASA Technical Memorandum 87150

Fatigue Crack Propagation of Nickel-Base Superalloys at 650 °C

(NASA-TM-87150) FATIGUE CRACK PROPAGATION
OF NICKEL-BASE SUPERALLOYS AT 650 DEG C
(NASA) 22 P HC AC2/HF A01 CSCL 11F

N86-12294

Unclas
G3/26 04809

J. Gayda, T.P. Gabb, and R.V. Miner
Lewis Research Center
Cleveland, Ohio

Prepared for the
Symposium on Low-Cycle Fatigue Directions for the Future
sponsored by the American Society for Testing and Materials
Bolton Landing, New York, September 30—October 4, 1985



NASA

FATIGUE CRACK PROPAGATION OF NICKEL-BASE SUPERALLOYS AT 650 °C

J. Gayda, T.P. Gabb, and R.V. Miner
National Aeronautics and Space Administration
Lewis Research Center
Cleveland, Ohio 44135

SUMMARY

The 650 °C fatigue crack propagation behavior of two nickel-base superalloys, René 95 and Waspaloy, were studied with particular emphasis placed on understanding the roles of creep, environment, and two key grain boundary alloying additions, boron and zirconium. Comparison of air and vacuum data showed the air environment to be detrimental over a wide range of frequencies for both alloys. More in depth analysis on René 95 showed at lower frequencies, such as 0.02 Hz, failure in air occurred by intergranular, environmentally-assisted creep crack growth, while at higher frequencies, up to 5.0 Hz, environmental interactions were still evident but creep effects were minimized. The effect of B and Zr in Waspaloy was found to be important where environmental and/or creep interactions were present. In those instances, removal of B and Zr dramatically increased crack growth and it is therefore plausible that effective dilution of these elements may explain a previously observed trend in which crack growth rates increased with decreasing grain size.

INTRODUCTION

Fatigue is usually the life limiting factor in modern aircraft turbine disks. Good resistance to fatigue crack propagation is important as well as resistance to crack initiation, since a crack once present must not propagate to failure between inspection intervals. Previous studies of several nickel-base, γ' strengthened disk alloys have shown that the advanced, fine grain, high strength alloys possess relatively poor fatigue crack propagation resistance at turbine disk rim temperatures, particularly when the fatigue cycle includes tensile dwell periods (refs. 1 and 2). Since these studies were conducted on commercial alloys rather than a specially designed series of alloys, it was not possible to conclude whether the poor fatigue crack propagation resistance of the advanced alloys was due to their generally finer grain size, higher strength, or possibly lower environmental resistance. More recent studies, in which grain size and strength were systematically varied for single superalloy compositions, have shown that fine grain size, but not high strength in itself, leads to accelerated crack growth at 650 °C (refs. 3 and 4). Further, it was shown that the high fatigue crack propagation rates of the fine grain alloys were associated with an intergranular mode of failure even at relatively rapid test frequencies, and that this mode did not occur in the absence of air. In dwell tests, failure was intergranular in both large and fine grain alloys, however, larger grain size still reduced the rate of crack propagation.

To gain a more detailed understanding of the rapid crack growth behavior of the fine grain alloys it is necessary to quantitatively gauge the relative importance of creep, fatigue, and environmental factors in the failure process. This question will be addressed in the first part of the present paper by

comparing crack growth behavior of René 95, a fine grain, high strength nickel-base superalloy, as a function of test frequency, dwell conditions, and environment.

To address why finer grain superalloys exhibit more rapid fatigue crack propagation, one mechanism relating grain size and grain boundary chemistry to fatigue crack propagation resistance will be assessed. The mechanism to be examined, which is essentially that proposed by Bain and Pelloux for creep crack propagation (ref. 5), is that since decreasing grain size increases grain boundary volume it effectively decreases the concentration of B and Zr at grain boundaries. Both elements are thought to enhance grain boundaries properties in superalloys and their effective dilution may therefore be responsible for the rapid intergranular fatigue crack propagation observed in fine grain superalloys. To test this hypothesis crack propagation tests were run on relatively fine grain Waspaloy with normal and reduced levels of B and Zr. The results of these tests and their relation to the fine grain nickel-base superalloys will be discussed in the second part of the present paper.

MATERIALS AND PROCEDURES

Creep-fatigue-environment study. - Crack growth tests designed to study the effects of creep, fatigue, and environmental interactions were conducted on a single nickel-base superalloy of current interest to the aerospace community, René 95. This alloy is typical of the current generation of fine grain, high strength nickel-base superalloys used as disk materials in the hot section of aircraft turbine engines. It is strengthened by the ordered intermetallic γ' phase and is produced by powder metallurgy technology.

Argon atomized powder having the composition listed in table I was used in the present study. This powder was hot isostatically pressed (HIP) at 1120 °C and 105 MPa for 3 hr producing essentially 100 percent density. The product was subsequently solution treated at 1120 °C for 1 hr, air cooled, and aged at 760 °C for 8 hr. The resulting microstructure has an average grain size of 8 μm and contains about 50 vol % of γ' precipitates about 0.1 μm in diameter plus a small amount of the MC carbide. Tensile properties for the René 95 studied are presented in table I and are typical of HIP René 95.

All crack growth data were generated using the compact tension specimen shown in figure 1 which was modified to maximize material usage. Both cyclic (R-ratio of 0.05) and static crack growth tests were run at 650 °C under load control using a closed loop servohydraulic test system equipped with an electric resistance furnace in a chamber which may be evacuated by a diffusion pump. Vacuum tests were run at a pressure between 1×10^{-5} and 1×10^{-6} torr. All other tests were run in laboratory air.

All compact tension specimens were precracked at room temperature in laboratory air at 20 Hz. A symmetric, triangular waveform was used for the cyclic crack growth tests, which were run at frequencies of 0.02, 0.33, and 5 Hz. Tests with a 120 sec dwell period at maximum load, but otherwise the same as the 0.33 Hz tests, were run to accentuate creep interactions. For the cyclic crack propagation tests, crack growth rates per cycle, da/dn , were monitored with a dc potential drop system described elsewhere (ref. 3) and were correlated with the stress intensity range, ΔK . For the static crack propagation tests, crack growth rates/time, da/dt , were also monitored with a dc potential

drop system and were correlated with the stress intensity factor, K . The K calibration curve for the modified specimen geometry was calculated using a boundary collocation scheme developed by Newman (ref. 6). At least two crack growth tests were run for every condition investigated herein.

Grain boundary chemistry study. - The effect of grain boundary chemistry on crack propagation rates was studied in a second nickel-base superalloy, Waspaloy. The use of HIP René 95 in this experiment was prohibited by the cost and time required to produce nonstandard compositions by powder metallurgy. However, the alloy chosen, Waspaloy could be produced with the available facilities by casting ingots of compositions desired and extruding them to obtain a fine grain microstructure.

Waspaloy is an older generation nickel-base superalloy with lower strength than René 95 primarily due to its lower γ' content. Nevertheless, work by Lawless (ref. 7) on Waspaloy and Gayda, Miner, and Gabb (ref. 4) on several nickel-base superalloys has shown that finer grain sizes tend to promote rapid, intergranular crack growth. Thus it was felt that the behavior of Waspaloy is representative of this class of superalloys and that Waspaloy was a suitable vehicle for studying the effects of grain boundary chemistry on crack growth behavior.

After several casting iterations, ingots with "normal" and low levels of B and Zr were obtained having otherwise nearly identical compositions as shown in table II. To refine the as-cast structure, these ingots were extruded at 1060 °C using a 6:1 reduction ratio. The extrusions were then solutioned at 1010 °C for 2 hr, forced air cooled, and then given a two step aging treatment of 845 °C for 4 hr and 760 °C for 16 hr. This heat treatment is similar to that used for commercial disk applications except the solution temperature was lowered slightly to prevent grain growth. The resulting microstructures for both compositions are shown in figure 2. The grain sizes are both about 40 μm . Both alloys were found to contain approximately 25 vol % γ' and a small amount of the MC and M_{23}C_6 carbides. The "normal" composition also contains a small amount of the M_3B_2 boride.

Crack growth tests were run on modified compact tension specimens previously described. Test temperature and procedures were identical to that already described for René 95. Cyclic crack propagation tests were run in air and vacuum at a frequency of 0.33 Hz with and without a 120 sec dwell at maximum load. The specimens were oriented so as to produce fracture perpendicular to the extrusion direction. The axes of tensile and creep specimens were also oriented to fracture in this plane.

RESULTS AND DISCUSSION

Creep-fatigue-environment study. - Fatigue crack growth data for the fine grain nickel-base superalloy René 95 are plotted in figures 3 and 4 for tests in air and vacuum, respectively. As seen in figure 3, crack growth rates in air varied by about one order of magnitude over the range of frequencies investigated. As expected, crack growth rates increased as test frequency decreases and increased dramatically for the 120 sec dwell test. In vacuum, figure 3, the crack growth rates showed a much smaller variation with frequency and the 120 sec dwell test is seen to be less damaging, especially at lower values of ΔK . Comparing tests of the same frequency in air and vacuum, crack growth

rates were clearly higher in air. This effect is seen to be most pronounced in the lower frequency tests. The increase of the crack growth rate in air was about a factor of two for the 5 Hz tests, but 50 times for the 120 sec dwell tests.

Creep crack growth rates for René 95 are presented in figure 5 for both air and vacuum. It may be seen that air enhanced the rate of creep crack growth almost thousand fold at this temperature. Further, crack growth rates in the two environments showed the greatest difference at lower values of K . Cyclic crack growth rates for the 120 sec dwell test in air and vacuum also differed most at low ΔK .

To analyse the effects of creep, fatigue, and environment in a more quantitative fashion the following scheme was adopted. First, the crack growth data at 5 Hz in vacuum was taken as the approximate rate of fatigue crack growth unaffected by creep or the air environment, $(da/dn)_f$. The validity of this assumption is supported by the near collapse of the fatigue crack growth data in vacuum at 5 and 0.33 Hz. This "pure" fatigue crack growth rate was then combined with the creep crack growth rate measured in air, da/dt , using a time integration method similar to that proposed by Saxena (ref. 8) to predict fatigue crack growth rates in air. The general form of this equation is shown below:

$$da/dn = (da/dn)_f + \int (da/dt) dt \quad (1)$$

The above expression is then evaluated at a given value of ΔK .

The first term in equation (1) was approximated by the Paris expression:

$$(da/dn)_f = B \Delta K^m = 1.07 \times 10^{-11} \Delta K^{2.95} \quad (2)$$

The integral in equation (1) was evaluated over one cycle from $t_1 = 0$ to $t_2 = (1/v) + t_{hold}$, where v is the frequency of the test and t_{hold} is the duration of any dwell.

Before the integral can be evaluated an expression for da/dt must be formulated. In this case the following expression was adopted:

$$da/dt = A k^n = 1.37 \times 10^{-16} k^{6.2} \quad (3)$$

This is merely a convenient form which accurately represents the creep crack growth data in air.

To perform the integration, an expression for K as a function of time within the cycle was then written based on the waveform in question, in this instance, a symmetric, triangular waveform with an optional dwell period at maximum load. The form of this expression and the mechanics of the integration are described in the appendix. The final relation is shown below:

$$da/dn = B \Delta K^m + A \Delta K^n [Z/(v(n+1)) + t_{hold}/(1-R)^n] \quad (4)$$

where

$$Z = (1 - R^{n+1})/(1 - R)^{n+1}$$

Evaluating the above expression at various values of ΔK for the 5, 0.33, and 0.02 Hz tests as well as the 120 sec dwell test yielded the plots shown in figure 6. Also shown for comparative purposes is the 5 Hz vacuum data used to approximate the "pure" fatigue crack growth rates.

Before proceeding, two points should be made about the time integration scheme used herein. First, the effect of creep crack growth is overestimated at low ΔK since the expression for the creep crack growth rate in air, equation (3), does not reflect the sharp decrease in da/dt below $K = 20 \text{ MPa}\sqrt{\text{m}}$ shown in figure 5. The effect is, however, relatively small on predicted fatigue crack growth rates at or above $\Delta K = 25 \text{ MPa}\sqrt{\text{m}}$, as the majority of the creep component in a fatigue cycle is incurred near K_{max} with the waveforms used in this study. Second, the time integration scheme as applied herein simply adds the creep component as measured in air to the "pure" fatigue component. The effects of environment are ignored except as they effect creep crack growth. Any interactive effects between the air environment and fatigue loading are not considered.

Examination of the predicted fatigue crack growth rates in air, figure 6, shows that simple addition of the air creep crack growth rates to the "pure" fatigue crack growth rate does not adequately explain the deleterious effect of the air environment at 5 and 0.33 Hz. At these higher frequencies the predicted crack growth rates are only slightly greater than the "pure" fatigue crack growth rates, especially at low ΔK . This suggests that there is an additional environmental effect in these fatigue tests which is not present in the creep crack growth tests run in air. Figure 7 shows that the 0.33 Hz tests exhibited an intergranular mode of failure indicating some form of environmental and/or creep damage is occurring, however the mode of failure was predominantly transgranular in the 5 Hz air tests with only a limited amount of intergranular failure evident.

While simple addition of the air creep crack growth rate to the "pure" fatigue crack growth rate underpredicts fatigue crack growth for the higher frequency tests it does much better for the cycles with a larger creep component, the 0.02 Hz and 120 sec dwell tests, shown in figure 6. In these tests it would appear that any acceleration in crack growth due to additional environmental interactions seen at higher frequencies is largely masked by the high crack growth rates produced by the large amount of creep crack growth in air. For example, the crack growth rate in air for the 120 sec dwell test is over two orders of magnitude greater than the "pure" fatigue crack growth rate due to the large amount of creep crack growth per cycle.

The effect of air on the high crack growth rates of the 0.02 Hz and 120 sec dwell tests in air is by no means minimal. This was demonstrated by the extremely low crack growth rates for the 120 sec dwell test in vacuum relative to that in air. Further the fracture modes of the air and vacuum 120 sec dwell tests were clearly different as seen in figure 7, that in air being decidedly more intergranular.

On the basis of these observations it appears that several failure mechanisms are operative in air run over the range of frequencies studied. At relatively high frequencies represented by the tests at 5 Hz, it is probable that the rate of crack growth outpaces the rate of oxygen penetration along grain boundaries, as evidenced by the transgranular fracture mode. Here the mild effect of air is probably related to environmental effects at or very

near the crack tip. These could include penetration and embrittlement by oxygen ahead of the crack tip at slip bands or oxidation of newly formed crack surfaces that would inhibit "rewelding."

At intermediate frequencies, represented by the tests at 0.33 Hz, the rate of oxygen penetration along grain boundaries is probably significant compared with the rate of crack propagation, as indicated by the more rapid, intergranular failure mode in air. Here the crack is propagating along grain boundaries apparently affected by air. It is possible that the grain boundaries have been embrittled by the actual depletion of oxide forming elements as proposed by Gell and Leverant (ref. 9), or more likely at this test temperature, just by the presence of oxygen diffused into the grain boundaries ahead of the crack tip.

At still lower frequencies, represented by the 0.02 Hz and the 120 sec dwell tests, the rate of oxygen penetration along grain boundaries must again be significant compared to the rate of crack propagation. However, there appears to be sufficient time in these cycles that the mechanism of crack growth resembles that occurring during static creep in an air environment as evidenced by the success in predicting crack growth rates at lower frequencies. Under these conditions oxygen may weaken or embrittle grain boundaries as previously described, or it may also increase creep rates, and therefore crack growth rates by altering cavitation kinetics as proposed by McLean (ref. 10).

Regardless of the mechanisms involved it is apparent that for René 95 fatigue crack growth rates for cycles with a substantial creep component are controlled by intergranular, environmentally assisted creep crack growth; while at higher frequencies fatigue crack growth rates are enhanced by the presence of the air environment with minimal creep interactions.

Grain boundary chemistry study. - Before examining the effects of B and Zr on crack growth in Waspaloy, a short discussion of tensile and creep properties is in order. As seen in table II, the 650 °C yield and ultimate tensile strengths were virtually unaffected by lowering B and Zr concentrations. The tensile elongation of the low B and Zr alloy was diminished but still acceptable at 12 percent, compared with 28 percent for the "normal" Waspaloy. The strength levels of both alloys were comparable to commercial Waspaloy as is the ductility of the "normal" alloy. The creep properties of the low B and Zr alloy, both rupture life and ductility, were also degraded as anticipated, figure 8.

The crack growth behavior in air and vacuum at 0.33 Hz for both alloys is shown in figure 9. Lowering the B and Zr level led to a threefold increase in crack growth rates in air. There was also a corresponding transition in fracture appearance to a more intergranular mode with lowered B and Zr levels, as seen in figure 10. In vacuum the crack growth rates of both alloys were nearly equivalent and less than that of either alloy in air. In addition, both alloys had a transgranular fracture appearance in vacuum, also shown in figure 10.

The crack growth behavior in air and vacuum for the 120 sec dwell test for both alloys are plotted in figure 11. In air the low B and Zr alloy had a crack growth rate more than one order of magnitude greater than the "normal" alloy. For both alloy the crack growth rate was greater than that observed at 0.33 Hz, although the effect in the low B and Zr alloy was much greater. For both alloys the mode of crack growth for the 120 sec dwell test in air was

predominantly intergranular. As in the 0.33 Hz tests, the crack growth rates of both alloys were suppressed in vacuum, but the crack growth rate of the alloy with lower B and Zr levels remained quite high, well above that obtained in air for the alloy with higher levels of B and Zr. Fracture in the low B and Zr alloy was predominantly intergranular for the vacuum dwell tests, however, that of the "normal" alloy was mixed as seen in figure 10.

These results clearly show that removing B and Zr adversely effects the crack growth behavior of Waspaloy when environmental and creep components are present alone or in combination. However, these two alloy additions have little effect on the "pure" fatigue crack growth process where failure is predominantly transgranular.

Comparison of alloy behaviors. - The effects of air and tensile dwell on the crack growth behaviors of René 95, and the two Waspaloy compositions are compared schematically in figure 12. The crack growth rates at $\Delta K = 30 \text{ MPa}\sqrt{\text{m}}$ for the 0.33 Hz and 120 sec dwell tests in both vacuum and air are plotted vertically at the four corners of the three-dimensional plot. The 0.33 Hz tests are the highest frequency tests conducted on all three alloys in vacuum and are taken as the "pure" fatigue crack growth behavior in this comparison.

It may be seen that the three alloys exhibit differing effects of air and dwell individually or in combination. However, the "pure" fatigue behavior of the three alloys is very similar and as previously stated removing B and Zr has little effect on crack growth behavior in this regime.

In vacuum, both René 95 and "normal" Waspaloy showed essentially no effect of the 120 sec tensile dwell. In the absence of air, creep loads have minimal effect on the crack growth behavior of these two alloys. However, Waspaloy with low B and Zr exhibited a more than tenfold increase in crack growth rates due to the application of the 120 sec dwell in vacuum, reflecting its low creep strength and ductility.

In air, all three alloys showed an increase in crack growth rates for both test cycles. However, the increase in crack growth rates was larger for René 95 and the Waspaloy with low B and Zr than for "normal" Waspaloy, particularly for the 120 sec dwell test. Low B and Zr levels were clearly detrimental to Waspaloy in both test cycles. This is unlike the findings of Floreen and Davidson (ref. 11) on the Ni-Fe-base superalloy they studied, NIMONIC PE16. It may be that PE16 is not as environmentally sensitive as the general class of Ni-base superalloys with higher fractions of γ' .

As the behavior of Waspaloy with low B and Zr somewhat mimics that of the fine grain René 95, support is given to a mechanism relating effective grain boundary composition to crack growth resistance such as that proposed by Bain and Pelloux (ref. 5). The effect of decreasing grain size in increasing fatigue and creep-fatigue crack growth rates of superalloys in air (refs. 2 and 3) may result, at least partly, from an effective dilution of the B and Zr concentration at grain boundaries.

Still, the effect of environment on René 95 is even more severe than that on Waspaloy with low B and Zr under creep-fatigue conditions. The high crack growth rates for Waspaloy with low B and Zr in the 120 sec dwell test in air appears to be as much due to basically poor creep behavior as to environmental

sensitivity. For René 95 the 120 sec dwell had no effect except in tests conducted in air. Thus, other factors, such as generally lower Cr concentration, probably also contribute to the enhanced crack growth rates of the advanced, fine grain superalloys like René 95 when creep, fatigue, and environment interactions are prevalent.

CONCLUSIONS

The results of this and previous studies show that rapid intergranular crack propagation observed in high strength, fine grain Ni-base superalloys, such as René 95, are a result of a strong environmental interaction. For low frequencies or cycles incorporating a tensile dwell, the damage mechanism is similar to that found in creep crack growth in air. Yet even for high frequency tests where creep interactions are minimal, the damaging effect of air is quite large. It has been shown previously that such environmental sensitivity is accentuated by fine grain microstructures. The present results on the effects of B and Zr concentrations in Waspaloy support the concept that a significant portion of the effect of fine grain size may be explained by the effective dilution of B and Zr concentration at grain boundaries due to an increase in grain boundary volume.

APPENDIX

To evaluate the creep component of crack growth, the integral is broken into three parts, the ramp up, the hold, and the ramp down, as shown below:

$$\int (da/da) dt = \int_0^{1/2v} AK^n dt + AK_{\max} t_{\text{hold}} + \int_{1/2v}^{1/v} AK^n dt^n$$

Since the first and the third term are numerically equivalent they may be combined as follows:

$$= 2 \int_0^{1/2v} AK^n dt + AK_{\max} t_{\text{hold}}$$

K is a linear function of time, t, as shown below:

$$K = 2v \Delta K t + K_{\min}$$

Substituting this expression for K in the integral one obtains:

$$= 2 \int_0^{1/2v} A(2v \Delta K t + K_{\min})^n dt + AK_{\max} t_{\text{hold}}$$

Expressing K_{\min} and K_{\max} in terms of ΔK and R, the load ratio, the following expression is obtained:

$$= 2 \int_0^{1/2v} A(2v \Delta K t + (R \Delta K)/(1 - R))^n dt + (A \Delta K^n t_{\text{hold}})/(1 - R)^n$$

The results of the integration are shown below:

$$= ((A \Delta K^n)/(vn + n))[(2vt + R/(1 - R))^{n+1}]_{t=0}^{t=1/2v} + (A \Delta K^n t_{\text{hold}})/(1 - R)^n$$

Note that ΔK is constant for a given cycle and has been removed from the integrand as ΔK^n . Evaluating the limits yields the following expression:

$$= [(A \Delta K^n)/(vn + n)][(1 + Q)^{n+1} - Q^{n+1}] + (A \Delta K^n t_{\text{hold}})/(1 - R)^n$$

where

$$Q = R/(1 - R)$$

This can be simplified by combining like terms to yield the second term of equation (4) in the text:

$$= A \Delta K^n [Z/(v(n+1)) + t_{hold}/(1-R)^n]$$

where

$$Z = (1 - R^{n+1})/(1 - R)^{n+1}$$

REFERENCES

1. Cowles, B.A., Sims, D.L., Warren, J.R., and Miner, R.V., Journal of Engineering Materials Technology, Vol. 102, No. 4, Oct. 1980, pp. 356-363.
2. Cowles, B.A., and Warren, J.R., "Evaluation of the Cyclic Behavior of Aircraft Turbine Disk Alloys," NASA CR-165123, National Aeronautics and Space Administration, Washington, D.C., Aug. 1980.
3. Gayda, J., and Miner R.V., Metallurgical Transactions A, Vol. 14A, No. 11, Nov. 1983, pp. 2301-2308.
4. Gayda, J., Miner, R.V., Gabb, T.P., in Superalloys 1984, M. Gell, ed., The Metallurgical Society of the AIME, Warrendale, PA, 1984, pp. 731-740.
5. Bain, K.R., and Pelloux, R.M., in Superalloys 1984, M. Gell, ed., The Metallurgical Society of AIME, Warrendale, PA, 1984, pp. 387-395.
6. Newman, J.C., in Fracture Analysis, ASTM STP-560. ASTM, Philadelphia, PA, 1974, pp. 105-121.
7. Lawless, B.H., "Correlation Between Cyclic Load Response and Fatigue Crack Propagation Mechanisms in the Ni-Base Superalloy Waspaloy," Masters Thesis, University of Cincinnati, Cincinnati, OH, 1980.
8. Saxsena, A., Fatigue of Engineering Materials and Structures, Vol. 3, No. 3, 1980, pp. 247-255.
9. Gell, M. and Leverant, G.R., in Fatigue at Elevated Temperatures, A.E. Garden, A.J. McEvily and C.H. Wells, eds., ASTM SPT-520, ASTM, Philadelphia, PA, 1973, pp. 37-67.
10. McLean, D., Metals Forum, Vol. 4, No. 1-2, 1981, pp. 44-47.
11. Floreen, S., and Davidson, J.M., Metallurgical Transactions A, Vol. 14A, No. 5, May 1983, pp. 895-901.

TABLE I. -- COMPOSITION AND 650 °C TENSILE
PROPERTIES OF RENÉ 95

Element	Weight percent	Tensile properties	
Cr	13.0	0.2 percent yield	1070 MPa
Co	8.2	Ultimate	1410 MPa
Mo	3.3	Elongation	13 percent
W	4.3		
Nb	3.6		
Ti	2.0		
Al	3.7		
C	0.047		
B	0.020		
Zr	0.025		
Ni	Balance		

TABLE II. - COMPOSITION IN WT% AND 650 °C TENSILE PROPERTIES OF THE TWO WASPALOY EXTRUSIONS

Element	Low B + Zr alloy	"Normal" alloy	Material	Yield 0.2 percent, MPa	Ultimate, MPa	Elongation, percent
Cr	20.8	20.7	Low B + Zr "Normal" alloy	810	1030	12
Co	12.8	12.8		770	1090	28
Mo	4.58	4.48				
Ti	3.53	3.55				
Al	1.81	1.79				
C	0.045	0.043				
B	0.001	0.025				
Zr	0.001	0.053				
Ni	Balance	Balance				

Technical drawing of a drop sensor assembly, showing dimensions in mm.

Top View Dimensions:

- Overall width: 25.1
- Overall height: 27.2
- Distance from left edge to center of top-left hole: 3.1
- Distance from left edge to center of bottom-left hole: 3.1
- Distance from left edge to center of top-right hole: 20.2
- Distance from left edge to center of bottom-right hole: 20.2
- Radius of top-right hole: 6.04
- Radius of bottom-right hole: 0.4
- Distance between centers of top-right and bottom-right holes: 14.5
- Distance from bottom edge to center of bottom-right hole: 13.6
- Distance from bottom edge to center of bottom-left hole: 3.1

Side View Dimensions:

- Overall height: 5.2
- Radius of top-right hole: 3.1

Labels:

- POTENTIAL DROP SENSING LEADS (pointing to the top-right and bottom-right holes)

ALL DIMENSIONS IN mm

Normal Waspaloy

Low B and ZR Waspaloy

14

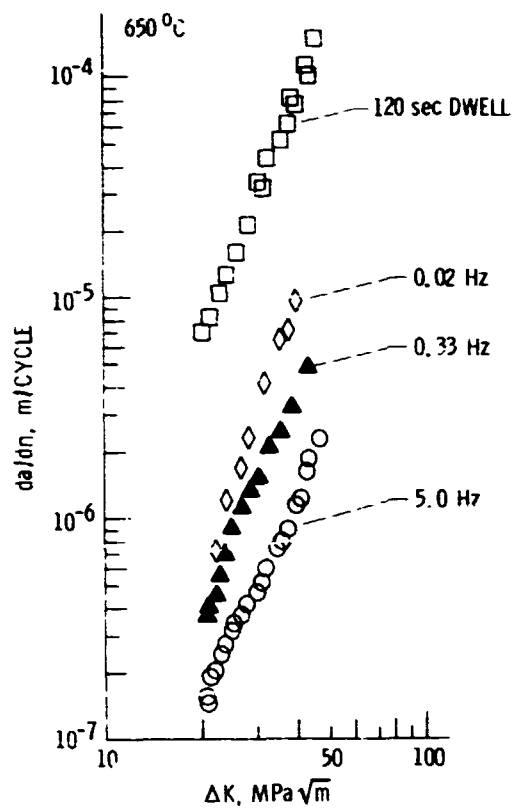


Figure 3. - Fatigue crack growth rates of René 95 tested in air.

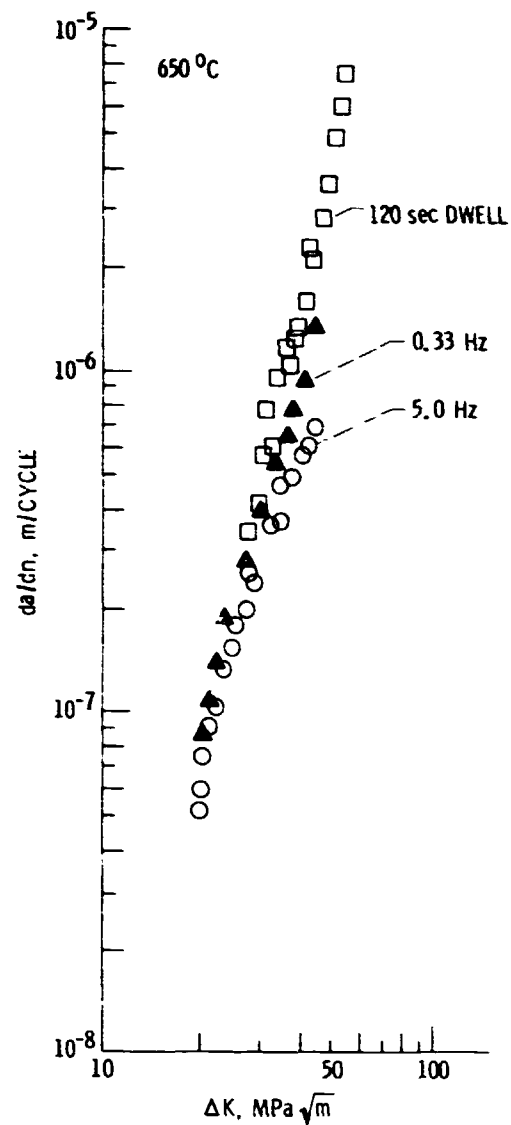


Figure 4. - Fatigue crack growth rates of René 95 tested in vacuum.

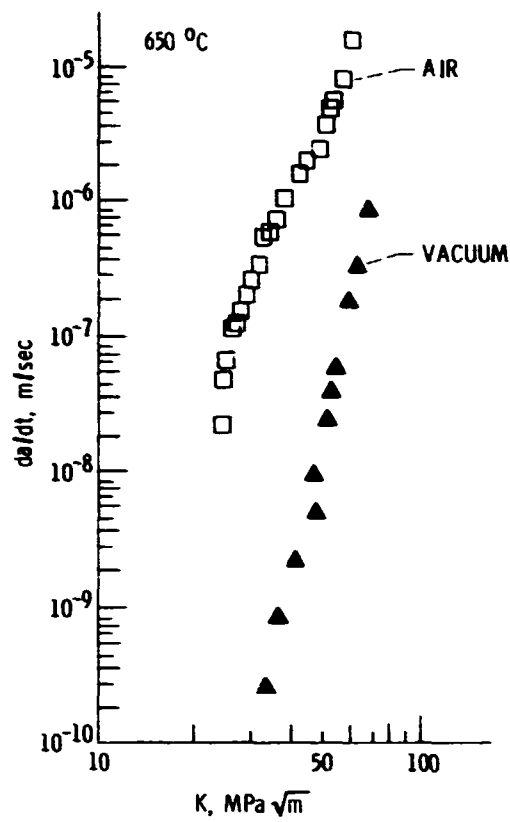


Figure 5. - Crack crack growth rates of René 95 in air and vacuum.

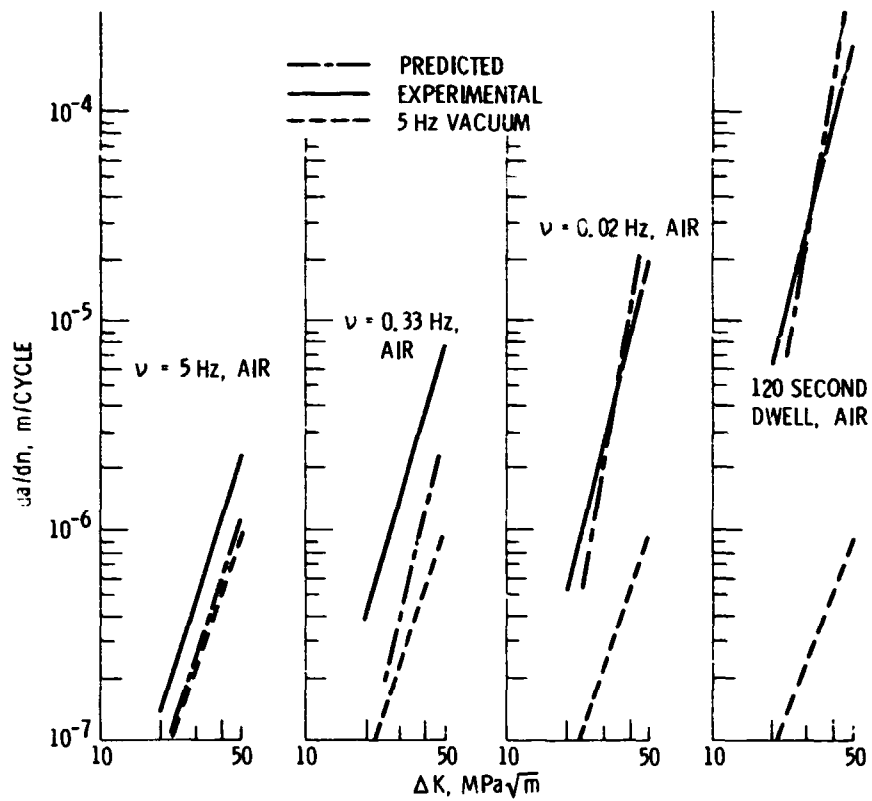


Figure 6. - A comparison of predicted and observed crack growth rates of René 95 at 650 °C.

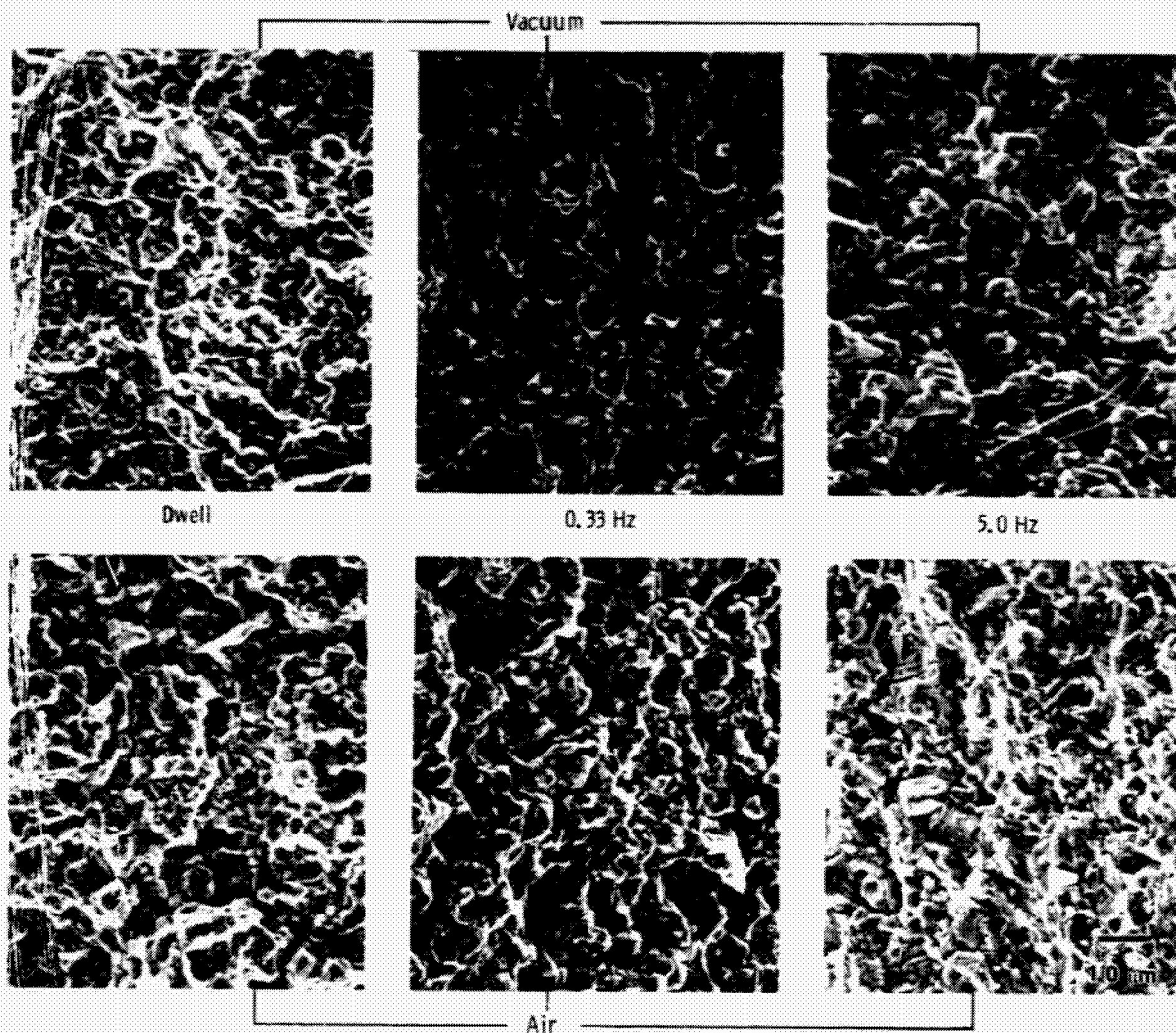


Figure 7. - Fracture modes observed in René 95 crack growth tests at 650 °C.

ORIGINAL PAGE IS
OF POOR QUALITY

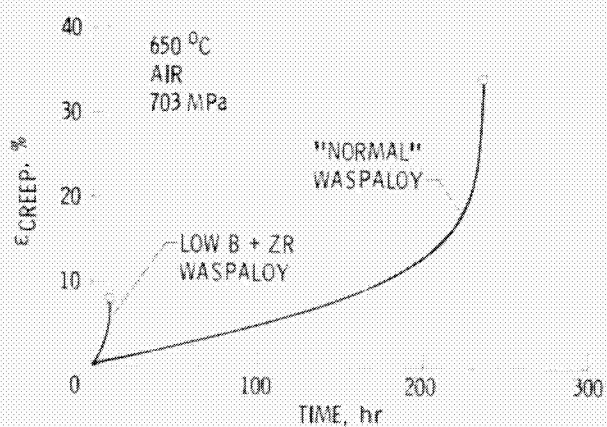


Figure 8. - Creep curves of the two Waspaloy compositions.

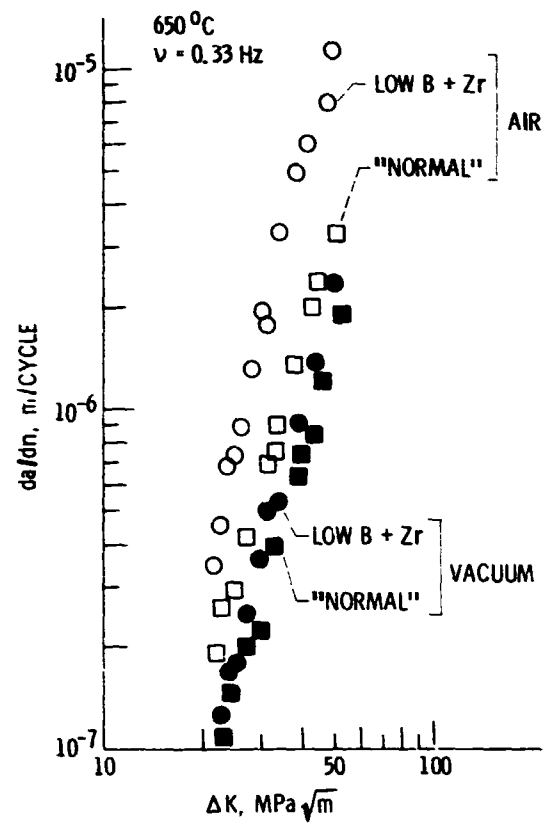


Figure 9. - Fatigue crack growth rates of the two Waspaloy compositions.

ORIGINAL PAGE IS
OF POOR QUALITY

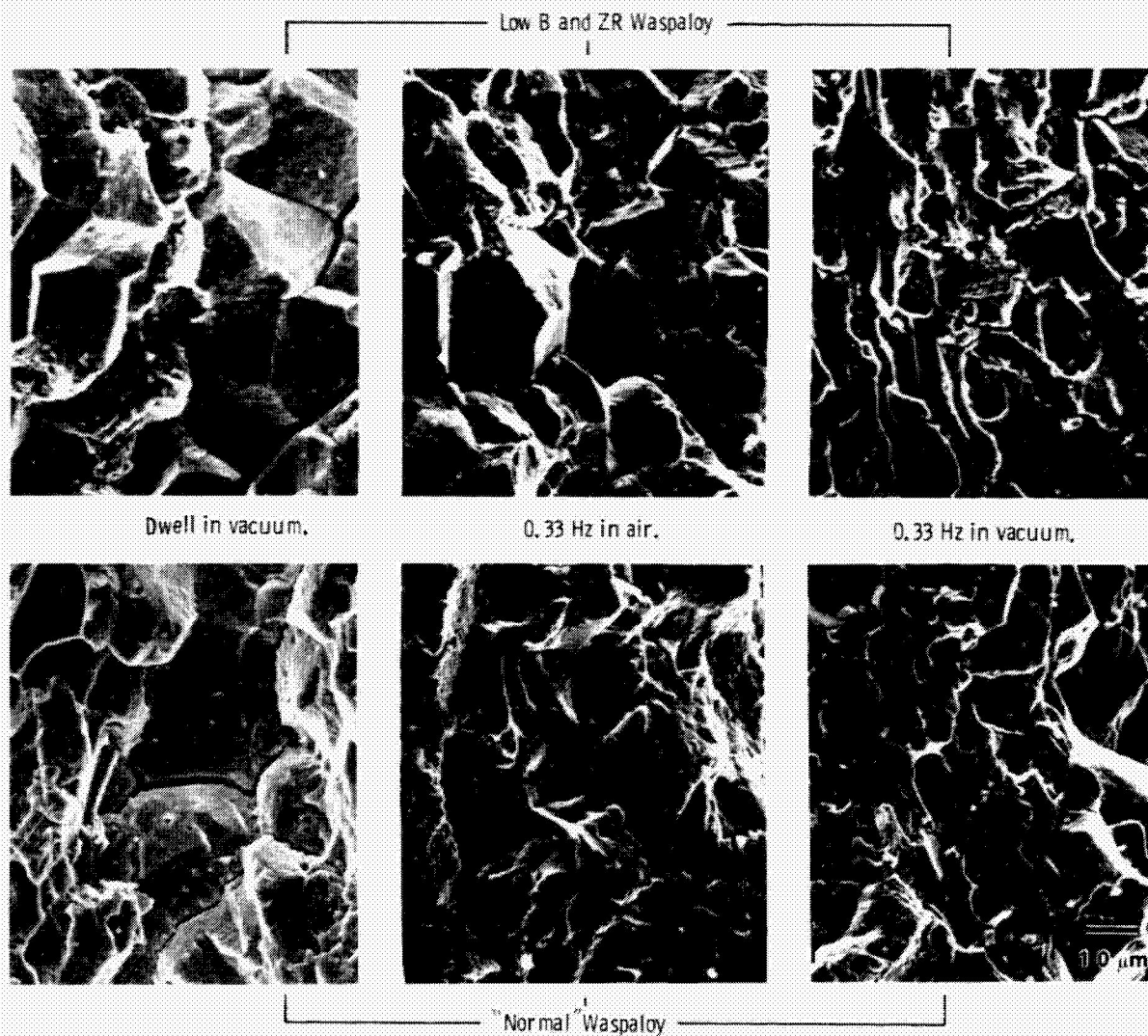


Figure 10. - Fracture modes observed in crack growth tests run at 650 °C on the two Waspaloy compositions.

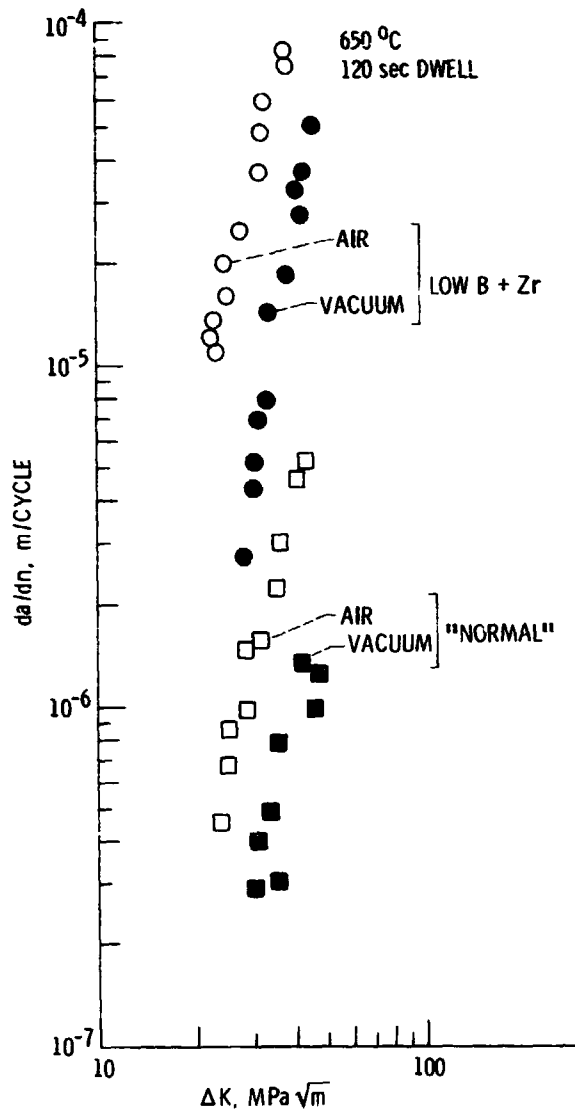


Figure 11. - Fatigue crack growth rates in the 120 second dwell tests run on the two Waspaloy compositions.

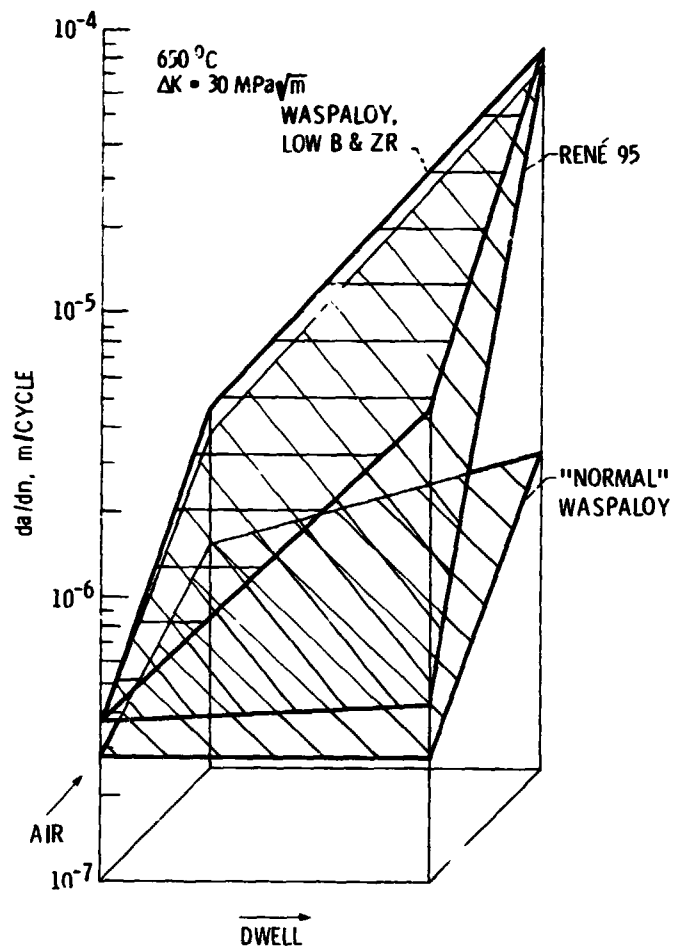


Figure 12. - A comparison of environmental and creep effects on fatigue crack growth behavior of Rene 95 and the two Waspaloy compositions.

1. Report No. NASA TM-87150		2. Government Accession No.		3. Recipient's Catalog No.	
4. Title and Subtitle Fatigue Crack Propagation of Nickel-Base Super-alloys at 650 °C				5. Report Date	
				6. Performing Organization Code 505-33-1A	
7. Author(s) J. Gayda, T.P. Gabb, and R.V. Miner				8. Performing Organization Report No. E-2778	
				10. Work Unit No.	
9. Performing Organization Name and Address National Aeronautics and Space Administration Lewis Research Center Cleveland, Ohio 44135				11. Contract or Grant No.	
				13. Type of Report and Period Covered Technical Memorandum	
12. Sponsoring Agency Name and Address National Aeronautics and Space Administration Washington, D.C. 20546				14. Sponsoring Agency Code	
15. Supplementary Notes Prepared for the Symposium on Low-Cycle Fatigue Directions for the Future sponsored by the American Society for Testing and Materials, Bolton Landing, New York, September 30 — October 4, 1985.					
16. Abstract The 650 °C fatigue crack propagation behavior of two nickel-base superalloys, René 95 and Waspaloy, were studied with particular emphasis placed on understanding the roles of creep, environment, and two key grain boundary alloying additions, boron and zirconium. Comparison of air and vacuum data showed the air environment to be detrimental over a wide range of frequencies for both alloys. More in depth analysis on René 95 showed at lower frequencies, such as 0.02 Hz, failure in air occurred by intergranular, environmentally-assisted creep crack growth, while at higher frequencies, up to 5.0 Hz, environmental interactions were still evident but creep effects were minimized. The effect of B and Zr in Waspaloy was found to be important where environmental and/or creep interactions were present. In those instances, removal of B and Zr dramatically increased crack growth and it is therefore plausible that effective dilution of these elements may explain a previously observed trend in which crack growth rates increased with decreasing grain size.					
17. Key Words (Suggested by Author(s)) Superalloys; Crack growth; Fatigue			18. Distribution Statement Unclassified - unlimited STAR Category 26		
19. Security Classif (of this report) Unclassified		20. Security Classif (of this page) Unclassified		21. No. of pages	
				22. Price*	